Suppression of Metabolic Activity Caused by Infantile Strabismus and Strabismic Amblyopia in Striate Visual Cortex of Macaque Monkeys

Agnes M. F. Wong, MD, PhD, FRCSC,[a,c] Andreas Burkhalter, PhD,[b] and Lawrence Tychsen, MD[a,b]

Introduction: Suppression is a major sensorial abnormality in humans and monkeys with infantile strabismus. We previously reported evidence of metabolic suppression in the visual cortex of strabismic macaques, using the mitochondrial enzyme cytochrome oxidase as an anatomic label. The purpose of this study was to further elucidate alterations in cortical metabolic activity, with or without amblyopia. ***Materials and methods:*** Six macaque monkeys were used in the experiments (four strabismic and two control). Three of the strabismic monkeys had naturally occurring, infantile strabismus (two esotropic, one exotropic). The fourth strabismic monkey had infantile microesotropia induced by alternating monocular occlusion in the first months of life. Ocular motor behaviors and visual acuity were tested after infancy in each animal, and development of stereopsis was recorded during infancy in one strabismic and one control monkey. Ocular dominance columns (ODCs) of the striate visual cortex (area V1) were labeled using cytochrome oxidase (CO) histochemistry alone, or CO in conjunction with an anterograde tracer ([H^3]proline or WGA-HRP) injected into one eye. ***Results:*** Each of the strabismic monkeys showed inequalities of metabolic activity in ODCs of opposite ocularity, visible as rows of lighter CO staining, corresponding to ODCs of lower metabolic activity, alternating with rows of darker CO staining, corresponding to ODCs of higher metabolic activity. In monkeys who had infantile strabismus and unilateral amblyopia, lower metabolic activity was found in (suppressed) ODCs driven by the nondominant eye in each hemisphere. In monkeys who had infantile esotropia and alternating fixation (no amblyopia), metabolic activity was lower in ODCs driven by the ipsilateral eye in each hemisphere. The suppression included a monocular core zone at the center of ODCs and binocular border zones at the boundaries of ODCs. This suppression was not evident in the monocular lamina of the LGN, indicating an intracortical rather than subcortical mechanism. ***Conclusion:*** Suppression of metabolic activity in ODCs of V1 differs depending upon whether infantile strabismus is alternating or occurs in conjunction with unilateral amblyopia. Our findings reinforce the principle that unrepaired strabismus promotes abnormal competition in V1, observable as interocular suppression of ODCs. (J AAPOS 2005;9:37-47)

Binocular vision is made possible by connections within the primary visual cortex (area V1) that allow sharing of information between the two eyes. These connections are necessary because the geniculocortical input into V1 is completely segregated into right eye and left eye ocular dominance columns (ODCs).[1,2] In normal monkeys, long-range horizontal projections in V1 are known to mediate binocular fusion by connecting right- and left-eye ODCs.[3,4] In monkeys with infantile strabismus, there is a paucity of horizontal connections,[3,4] thus accounting for their abnormal binocular behaviors.

Suppression is a major sensorial abnormality in humans and monkeys with infantile strabismus. Visual inputs may be suppressed from one eye continuously (causing unilateral amblyopia) or, more commonly in infantile strabismus, from each eye alternately 50% of the time (alternate fixation).[5,6] In normal adult animals, horizontal connections between ODCs can mediate suppression when conflicting stimuli activate neurons in neighboring ODCs.[7,8] Our group previously reported evidence of suppression of ODCs in macaques who had natural alternating infantile esotropia, using the metabolic enzyme cytochrome oxidase

From the Departments of Ophthalmology and Visual Sciences[a], and Departments of Anatomy and Neurobiology,[b] Washington University School of Medicine, St. Louis, MO, USA; and Department of Ophthalmology and Vision Sciences, University of Toronto, Toronto, Ontario, Canada[c]

This work was supported by NIH Grant EY10214 (A.B. and L.T.) and a New Investigator Award from the Canadian Institutes of Health Research (A.W.).

The authors have no financial conflict of interest regarding the subject matter in this article.

Submitted April 22, 2004.

Revision accepted September 17, 2004.

Reprint requests: Lawrence Tychsen, MD, Room 2, South 89, St. Louis Children's Hospital, Washington University School of Medicine, One Children's Place, St. Louis, MO 63110.E-mail: tychsen@vision.wustl.edu.

1091-8531/2005/$35.00 + 0

doi:10.1016/j.jaapos.2004.09.004

Journal of AAPOS
Volume 9 Number 1 February 2005

TABLE 1. Visual and ocular motor characteristics of the six macaque monkeys used in the study

Animal/Sex/ Age (species)	Ocular History	Eye Alignment	Visual Acuity	Fixation Preference	Refractive Error	Latent Nystagmus	Pursuit/OKN Asymmetry
ZY/F/7 yr (*M. mulatta*)	Naturally strabismic	LET: 21 deg	RE: 12.80 cpd LE: 8.67 cpd (SSVEP)	RE (LE amblyopia)	RE: −0.25 LE: +2.00 + 1.00 × 170	Yes	Yes
PY/M/6 yr (*M. mulatta*)	Naturally strabismic	LXT: 14 deg	RE: 9.47 cpd LE: 6.57 cpd (SSVEP)	RE (LE amblyopia)	RE: +1.00 + 1.25 × 115 LE: −1.50 + 0.50 × 65	Yes	Yes
JE/F/8 yr (*M. nemistrina*)	Naturally strabismic	ET: 15 deg	RE: FFM LE: FFM	Alternating	RE: +4.00 LE: +3.00	Yes	Yes
RD/M/3 yr (*M. mulatta*)	Alternating occlusion-induced strabismus	ET: 5 deg	RE: 10.3 cpd LE: 9.6 cpd (FPL)	Alternating	RE: +2.25 LE: +1.25 + 1.00 × 180	Yes	Yes
ZN/M/8 yr (*M. mulatta*)	Normal	Orthophoric	RE: 15.3 cpd LE: 17.4 cpd (SSVEP)	Orthotropic	RE: +0.50 LE: +1.00	No	No
RF/M/3 yr (*M. mulatta*)	Normal	Orthophoric	RE: 10.5 cpd LE: 9.2 cpd (FPL)	Orthotropic	RE: +3.00 + 1.00 × 124 LE: +2.00	No	No

cpd = cylce per degree; *ET* = esotropia; *FFM* = fix, follow, maintain; *FPL* = forced-choice preferential looking; *LE* = left eye; *OKN* = optokinetic nystagmus; *RE* = right eye; *SSVEP* = spatial sweep VEP; *XT* = exotropia.

(CO).[3,9] The abnormality was shown subsequently to be a general anatomic feature of abnormal binocular activity in area V1, caused by either strabismus or amblyopia. The abnormality was apparent in V1 of macaques who had experimentally induced, infantile esotropia without amblyopia,[9,10] in a monkey with natural anisometropic amblyopia without strabismus,[11] and in monkeys in whom unilateral exotropia was induced in adulthood.[12]

The goal of this study was to further elucidate alterations in CO activity in the cortex of strabismic macaques, including animals—not reported previously—with combined infantile strabismus and strabismic amblyopia.

MATERIALS AND METHODS

Animals

Four strabismic and two normal macaque monkeys were used in the experiments (Table 1). Two of the four strabismic monkeys (JE and ZY) were documented to have naturally occurring, nonparalytic esotropia (nat-ET) with onset before 4 to 6 weeks of age. The third strabismus monkey (PY) had naturally occurring, nonparalytic infantile-onset exotropia (nat-XT). The fourth strabismic monkey (RD) had strabismus induced by rearing under conditions of alternating monocular occlusion (ao-ET). Within 1 hour of birth, an opaque soft contact lens was inserted into one eye. The contact lens was alternated from eye to eye every 24 hours until age 9 months. Contact lens loss was carefully monitored throughout the day and night, with replacement lenses promptly reinserted, such that less than 0.5% of the animal's visual experience during these 9 months was binocular. Visual acuity and eye alignment testing was performed at weekly intervals during the first 3 months of life and at monthly intervals thereafter. From age 9 months to euthanasia at age 3 years, no contact lens was worn. Funduscopic examinations showed no evidence of ocular albinism or optic neuropathy. Two monkeys (ZN and RF), with normal binocular vision, served as controls. The (cycloplegic) refractive error of each animal is listed in Table 1. Strabismic monkeys JE and RD had measurement of average ODC widths and the observation of "spontaneous" CO stripes reported previously in a basic science journal.[9] Convergence eye movement data in normal monkey ZN were included in a previous report.[13] The experimental protocol was approved by Washington University Animal Care and Use Committee.

Visual Acuity Testing

Visual acuity (without correction for any refractive error) was quantified in five of the six monkeys and was assessed using Fix, Follow, Maintain criteria in one animal (monkey JE).[14] Monkeys RD and RF had grating acuity measured in infancy by means of a forced-choice preferential looking method (FPL).[15] The monkey was held in front of a stimulus field which contained a high-contrast square-wave grating on either the left or the right side. An observer, who was blind as to the position of the stimulus and the stripe width on every trial, viewed the monkey on a video monitor. On the basis of the monkey's orienting behavior and eye movements, the observer made a judgment as to the stimulus position, left or right. The observer was required to maintain a criterion performance of at least 80% correct on the largest stripe width for any single session. Acuity estimates were based on 20 to 40 trials at each of four stripe widths near resolution threshold. The stripe width was chosen so that performance on the narrowest was expected to be near chance and perfor-

TABLE 2. Anatomic labeling methods and CO stripe patterns in the six monkeys

Animal	Ocular History	ODC Labeling Method	CO ODC Stripe Pattern	Ocularity of CO ODC Stripes
ZY	Naturally strabismic	RE injected with proline 10 days before euthanasia; CO labeling	Thin dark Wide pale	Dark = RE (preferred eye) Pale = LE (amblyopic eye)
PY	Naturally strabismic	RE injected with proline 10 days before euthanasia; CO labeling	Thin dark Wide pale	Dark CO stripes = RE (preferred eye) Pale CO stripes = LE (amblyopic eye)
JE	Naturally strabismic	RE injected with WGA-HRP 48 hr before euthanasia; CO labeling	Thin dark Wide pale	Dark = Contralateral eye (nasal retina) Pale = Ipsilateral eye (temporal retina)
RD	Alternating occlusion-induced strabismus	CO labeling	Thin dark Wide pale	Double-labeling not performed
ZN	Normal	LE laser 1 wk before euthanasia; CO labeling	Normal width: dark Normal width: pale	Dark = Intact eye Pale = Deafferented eye
RF	Normal	LE laser 1 wk before euthanasia; CO labeling	Normal width: dark Normal width: pale	Dark = Intact eye Pale = Deafferented eye

mance on the widest was expected to be near 100%. Probit analysis[16] was applied to these data to obtain estimates of acuity, which was defined as the stripe width that would result in 75% correct performance.

In monkeys ZY (nat-ET), PY (nat-XT), and ZN (normal), visual acuity was measured using spatial sweep visually evoked potentials (SSVEP).[17] Electrodes were placed over the occipital scalp using a standard arrangement. Vertical sine-wave gratings were presented in individual trials as a 10-second spatial frequency sweep which spanned the acuity limit. The amplitude and phase of the second harmonic response were extracted by discrete Fourier analysis. The VEP amplitude versus spatial frequency function showed narrow spatial frequency tuning with amplitude peaks at one or more spatial frequencies. A linear regression line was drawn from the highest spatial frequency peak in the VEP amplitude to the spatial frequency at which the regression line crossed zero microvolts (considered background EEG level). This value was taken as the estimate of VEP acuity. Amblyopia was defined as an interocular difference of greater than one-half octave (by either FPL or SSVEP).

Stereopsis Testing

Stereoacuity testing was performed on monkeys RD and RF. A forced-choice preferential looking technique was used to present random-dot stereograms.[18] A set of stereograms reproduced in the form of vectograph transparencies was used as stimuli. Dichoptic viewing was achieved by a combination of polarizing material embedded into the vectograph transparencies, and polarizing filter goggles in front of the monkey's eyes. The stereograms were placed in pairs consisting of a stereogram of a given disparity, along with a stereogram of zero disparity. The monkey was observed and a judgment was made, based on the monkey's preference as inferred from eye and head movements, as to whether the disparate stereogram was on the left or the right. A session was ended when qualitative evaluation of the data collected revealed that performance on the largest disparities tested was near perfect, performance on the smallest disparities tested was near chance, and intermediate disparities had values near 75% correct. Estimation of threshold disparity was done by subjecting each data set to statistical probit analysis.[16]

Ocular Motor Recording

Eye alignment and fixation preference were tested initially in each monkey using a video Hirschberg method. In monkeys JE, RD, and RF, video recordings were used to document the presence of fixation (latent) nystagmus and to measure horizontal pursuit and optokinetic nystagmus (OKN), under conditions of monocular viewing. In monkeys ZY, PY, and ZN, binocular scleral search coils and a head restraint were implanted using techniques described in detail elsewhere,[19] and eye movements were recorded using the magnetic search coil technique.[19-21]

Neuroanatomic Methods

Table 2 lists the alternative techniques used to label ODCs in each animal.

Intraocular Tracer Injection. In strabismic monkeys ZY and PY, ODCs were labeled using the transneuronal autoradiography protocols of Wiesel and Hubel[22] and Horton et al.[12] The radioisotope was prepared by reconstituting 2 mCi of L-[2,3,4,5-^{3}H]proline (specific activity, 102 to 106 Ci/mmol; Amersham, Arlington Heights, IL) in 20 μL sterile balanced salt solution. In strabismic monkey JE, ODCs were labeled using wheat germ agglutinin-horseradish peroxidase (WGA-HRP).[9]

The monkey was sedated with ketamine hydrochloride (10 mg/kg IM) and atropine (0.04 mg/kg IM). A topical anesthetic drop (proparacaine) was applied to numb the surface of the eye. The pupils of both eyes were dilated using mydriatic (neosynephrine 2.5% and cyclopentolate 1%) drops. The eye to be injected was gently massaged to lower intraocular pressure. The eye was rotated medially and stabilized with a Castroviejo forceps so that the sclera overlying the pars plana could be visualized (in the typical adult monkey this is 2 mm posterior to the corneoscleral limbus). The beveled 27-gauge needle on a Hamilton

syringe was introduced through the pars plana into the mid-vitreous cavity. The solution ([^{3}H]proline or WGA-HRP) was injected over 1 minute to allow for diffusion within the vitreous. The needle was withdrawn from the self-sealing scleral wound and the fundus was examined with an indirect ophthalmoscope to verify absence of retinal trauma. The animal was awakened and returned to its home cage. The label was transported anterogradely, transsynaptically from eye to brain over a survival time of 10 days for [^{3}H]proline, and 48 hours for WGA-HRP.

Laser Deafferentation. In the normal animals, ZN and RF, the left eye was deafferented using a laser.[4,9,23,24] The deafferentation caused down regulation of CO activity in neurons dominated by input from that eye. The monkey was sedated with ketamine hydrochloride (10 mg/kg IM) and atropine (0.04 mg/kg IM). The pupils were dilated using mydriatic drops. An indirect-ophthalmoscope fitted with a diode laser (Iris Medical, Inc) was used to apply ~150 to 200 spot burns (200 mw, 200 ms per burn) to the optic disk. The method of application and laser intensity were the same as that used to treat humans with retinal disorders. The laser did not affect the ocular media and caused no obvious discomfort. Atropine 1% and Cortisporin ointment were instilled on the conjunctiva of both eyes. The animal was awakened and returned to its home cage.

Euthanasia and Brain Perfusion. The animals were anesthetized using ketamine, and a lethal dose of sodium pentobarbital (120 mg/kg IM) was administered. After pronounced slowing of the EKG was evident, the chest was opened to expose the heart. A cannula was inserted in the left ventricle and 1 L normal saline followed by 1 L 2% paraformaldehyde in 0.1 mol/L phosphate buffer was infused by an electric pump. The cerebral hemispheres were then removed from the cranium. The brainstem with the attached lateral geniculate nuclei (LGN) was removed and immersed in a separate container of fixative. The skull was preserved for examination of orbital structures.

Tissue Processing. The leptomeninges over the occipital lobes was peeled back and the sulci opened. The brain was photographed and sketched for purposes of orientation and scale. The cortex anterior to lunate sulcus was removed and the white matter underlying striate cortex was carefully scraped away using blunt dissecting instruments.[25,26] The resulting sheet of folded cortical matter was flattened by gentle pressure under a glass petri dish. Relieving cuts were made to flatten tissue that appeared too highly folded, thus reducing the striate cortex to a number of blocks small enough for convenient sectioning. The blocks were then postfixed for 1 to 2 hours and subsequently immersed overnight in 0.1 mol/L phosphate-buffered 30% sucrose at 4°C. The blocks were frozen rapidly on dry ice and cut into 40-μm sections on a freezing microtome in a plane parallel to the pial surface. The midbrain, thalami, and LGN were cut in transverse/coronal sections.

Autoradiography. To reveal ODCs labeled with [^{3}H]proline, sections were mounted on gelatinized slides, dried, and dipped into NTB-2 emulsion (Eastman Kodak, Rochester, NY). The autoradiographs were exposed for 10 weeks, developed (D19 developer, Kodak), and digitally photographed for computer imaging using Photoshop 6.0 (Adobe Systems, San Jose, CA).

WGA-HRP Histochemistry. To reveal ODCs labeled with WGA-HRP, floating sections were processed for tetramethylbenzidine (TMB) histochemistry by using the Gibson et al[27] modification of the protocol by Mesulam.[28] Stained tissue was mounted on gelatin-coated slides, dehydrated in ethanol, cleared in xylene, and coverslipped with DPX.

CO Histochemistry. Mounted sections were stained using the protocol of Tootell et al.[29] When stained, the sections were run through an ascending series of alcohols, followed by xylenes, and then coverslipped with DPX.

CO Densitometry. Quantitative estimates of inequalities in CO histochemistry staining were derived by densitometry[30] in strabismic monkeys RD and JE and normal monkey ZN. Measurements were obtained using a Wild stereomicroscope fitted with a Nikon UFX-II photometer and halogen lamp illumination. CO-dark and CO-pale ocular dominance stripes of layer 4C were identified at ×125 magnification, and a 250-micron-diameter aperture was positioned at the center of the stripe. A minimum of 10 densitometry readings were obtained from subsets of pale and dark stripes. The background density (measured over an area of slide with no tissue) was subtracted electronically. Lighting conditions were held constant for each section. Mean density for CO-pale stripes was divided by mean density for CO-dark stripes to obtain a light-dark ratio.

RESULTS

Visual Acuity and Amblyopia

Strabismic monkeys JE (nat-ET) and RD (ao-ET) alternated fixation from eye to eye, with no evidence of amblyopia by fixation preference criteria. The development of grating acuity in ao-ET monkey RD is plotted in Figure 1. Acuity rose systematically in each eye during the first 5 months of life and stayed above the 95% confidence interval for normal infant monkeys (including that of normal monkey RF). As listed in Table 1, both ao-ET monkey RD and normal monkey RF achieved acuities above 9 cycles per degree (cpd) in each eye, as did normal monkey ZN.

In contrast, strabismic monkeys ZY (nat-ET) and PY (nat-XT) displayed a consistent right eye fixation preference due to amblyopia in the left eye in both animals. For monkey ZY (nat-ET), acuity was 12.80 cpd in the preferred right eye and 8.67 cpd in the amblyopic left eye. For monkey PY (nat-XT), acuity was 9.47 cpd in the preferred right eye and 6.57 cpd in the amblyopic left eye. These two animals with strabismic amblyopia also had mild anisome-

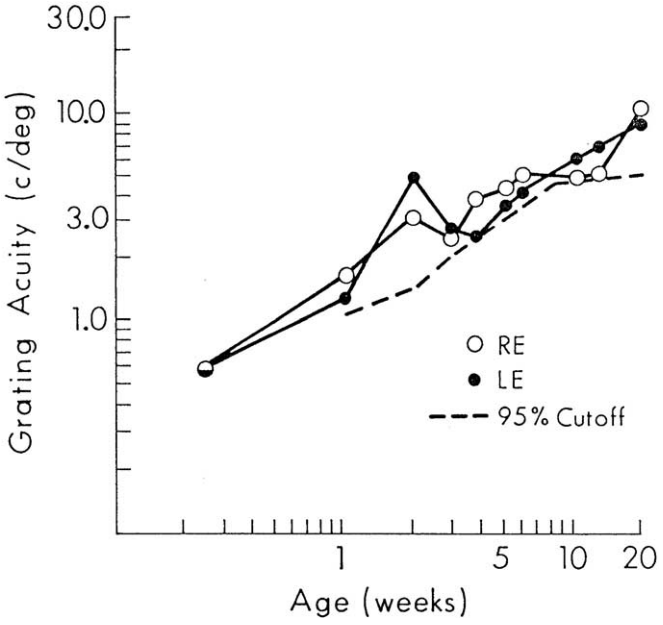

FIG 1. The development of grating acuity using the FPL technique in ao-ET monkey RD's right and left eyes. Dotted line indicates lower limit of 95% confidence interval for control infant macaques, including monkey RF.

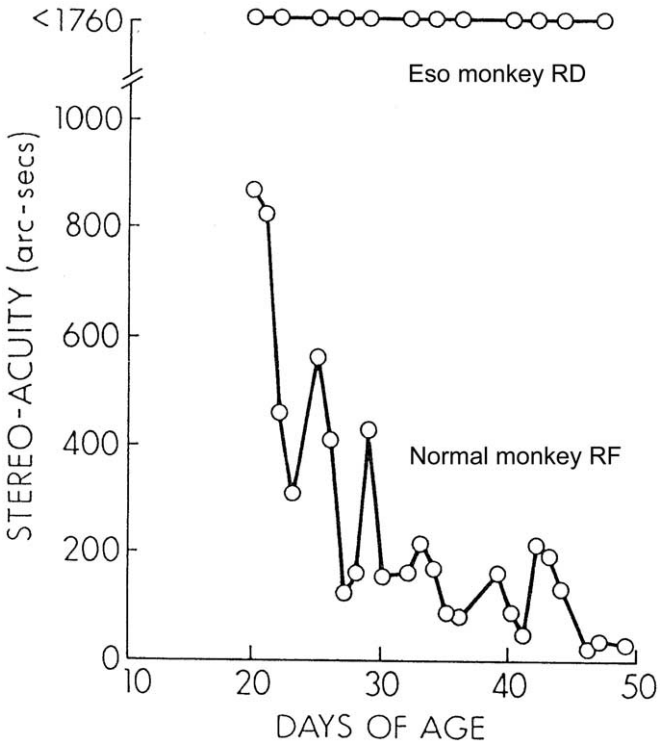

FIG 2. The development of stereopsis using the FPL technique in ao-ET monkey RD compared with control monkey RF.

tropia (Table 1). In monkey ZY, the amblyopic eye was mildly hyperopic, but in monkey PY the amblyopic eye was mildly myopic.

Stereopsis and Motor Fusion (Vergence) Disparity Sensitivity

Stereopsis was tested from birth to greater than 9 weeks in ao-ET monkey RD and normal monkey RF. As shown in Figure 2, ao-ET monkey RD remained stereoblind, whereas normal monkey RF developed adult-like levels of stereopsis (~40 arc sec) by age 6 weeks. The postnatal development of stereopsis in this monkey was typical for normal infant macaques.[18]

Binocular disparity sensitivity was assessed in nat-ET monkey ZY and normal monkey ZN using large-field random dot stimuli to evoke short-latency fusional vergence eye movements.[31] Fusional vergence was robust in normal monkey ZN but absent in nat-ET monkey ZY. Neither stereopsis nor disparity vergence was tested in nat-ET monkey JE or nat-XT monkey PY. The presence of a large-angle, constant strabismus implies strongly that these animals were also stereoblind.

Ocular Motor Abnormalities

Constant, concomitant esotropia of 15 to 21 deg was documented in nat-ET monkeys JE and ZY (Table 1). A constant exotropia of 14 deg was found in nat-XT monkey PY. Alternating occlusion monkey RD had a constant, small angle (~5 deg) or micro-esotropia. Control monkeys ZN and RF were orthophoric.

Each of the four strabismic monkeys exhibited other ocular motor deficits that typify infantile strabismus in humans.[32] When viewing monocularly (ie, one eye covered), they showed latent (fusion maldevelopment) nystagmus, a nasotemporal asymmetry of horizontal smooth pursuit, and a naso-temporal asymmetry of OKN (Table 1). Control monkeys ZN and RF displayed none of these abnormalities.

Metabolic Labeling of Striate Cortex

Abnormal metabolic activity, as revealed by CO histochemistry, was evident in area V1 in each of the strabismic monkeys. The abnormality was apparent as alternating rows of darker and lighter staining ODCs at the input later of primary cortex, lamina 4C. Figure 3 is a photomicrograph taken at low power, showing a tangential section through flattened V1 in nat-ET monkey ZY at a retinotopic eccentricity ~ 5 deg. The majority of the section is confined to layer 4C, with a paler oval region intersecting layer 4B (upper left), and a pale triangular region with a few dark patches (top right corner) traversing into layers 2/3. Note the thin dark stripes in layer 4C (four of which are marked by the arrows), alternating with wider, pale stripes. The centers of the dark stripes were 400 to 500 microns apart, or the normal width separating the centers of ODCs. The dark stripes corresponded to ODCs, which stained intensely for CO (higher premortem metabolic activity), and the pale stripes corresponded to rows of

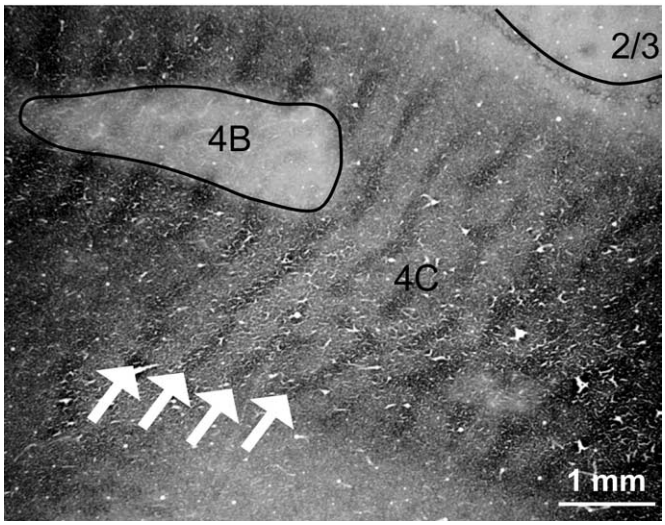

FIG 3. Tangential section through flattened V1 in naturally esotropic monkey ZY who had strabismic amblyopia of the left eye. The majority of the section is confined to layer 4C, with a paler oval region intersecting layer 4B (left side), and a quasi triangular region (top right) traversing into layers 2/3. Note the thin dark stripes in layer 4C (four of which are marked by the arrows), alternating with wider, pale stripes. The centers of the dark stripes are 400 to 500 microns apart, or the normal width separating the centers of ODCs. The dark stripes correspond to ODCs of the preferred right eye, which stain intensely for CO (higher premortem metabolic activity). The pale stripes correspond to ODCs of the amblyopic left eye which stain poorly (lower metabolic activity).

ODCs, which stained poorly (lower metabolic activity). This abnormality—dark and light rows of CO-stained ODCs—does not occur in monkeys with normal binocular vision.[33,34] In normal primates, layer 4C stains homogeneously and ODCs are not visible (to make layer 4C ODCs visible using CO, a normal monkey must have one eye deafferented).[3,9,24]

In monkey V1, the central 10 deg of the visual field is represented on the external surface (or operculum) of the occipital lobe, whereas visual field eccentricities beyond 10 deg, including the optic disk representation and the monocular crescent, are represented within the depths of the calcarine (mesial) sulcus.[24,35-37] In sections through calcarine V1, the optic disk representation was identifiable as an interruption in the ODC stripe pattern corresponding to those ODCs driven by the nasal hemiretinae (ie, contralateral eye) in each V1. The monocular crescent in each V1 also corresponds to ODCs driven exclusively from the nasal hemiretinae. The staining pattern of these landmarks, in addition to anterograde labeling by injection of [^{3}H]proline into the right eye (Table 2), allowed us to determine which ODCs belonged to the right versus left eye in each hemisphere. The darkly staining ODCs in Figure 3 belonged to the preferred (dominant) right eye in monkey ZY. The pale ODCs represented the amblyopic, left eye. Inspection of sections through the opercular and calcarine cortex disclosed that both the central and the peripheral retinotopic regions of V1 exhibited the ODC inequality of Figure 3.

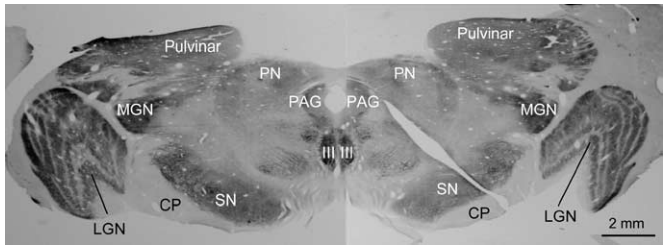

FIG 4. CO-stained section through the midbrain at the level of the oculomotor (third cranial nerve) nuclei. The left and right lateral geniculate nuclei (LGN) can be seen to contain six distinct curvilinear neuronal layers, from layer 1 on the concave, ventral surface to layer 6 on the convex, dorsal surface. Lamina 1, 4, and 6, representing the contralateral eye, and lamina 2, 3, and 5, representing the ipsilateral eye, stain intensely and equally for CO, without evidence of the CO inequality detected in V1. LGN, lateral geniculate nucleus; MGN, medial geniculate nucleus; PN, pretectal nuclei; PAG, periaqueductal gray; III, oculomotor nucleus; SN, substantia nigra; CP, cerebral peduncle.

Examination of the LGN in nat-ET monkey ZY (as well as PY and JE) revealed that the metabolic abnormality caused by strabismus was localized to the visual cortex and was not a subcortical-brainstem pathology. The left and right LGN of monkey ZY (Figure 4) are evident as the cap or crescent-shaped bodies at the lateral extents of this CO-stained section through the midbrain at the level of the oculomotor (third cranial nerve) nuclei. Each LGN can be seen to contain six distinct curvilinear neuronal layers, from layer 1 on the concave, ventral surface to layer 6 on the convex, dorsal surface.[38,39] Lamina 1, 4, and 6, representing the contralateral eye, and lamina 2, 3 and 5, representing the ipsilateral eye, stained intensely and equally for CO, without evidence of the CO inequality present at the level of V1.

A similar pattern of ODC staining was observed in sections through V1 of nat-XT monkey PY. Figure 5A shows a [^{3}H]proline-labeled section through layer 4C in the opercular cortex (corresponding to ~7 deg eccentricity). [^{3}H]proline was injected into the preferred right eye and transported anterogradely to anatomically labeled ODCs driven by that eye, independent of any CO activity. The ODCs of the injected right eye appeared as pale stripes, as indicated by the white arrows. Note that the [^{3}H]proline-labeled and [^{3}H]proline-nonlabeled ODCs, belonging to the preferred right eye, and amblyopic left eye, respectively, were of equivalent normal width, ie, 400 to 500 microns. An adjacent section stained with CO is shown in Figure 5B. The "metabolic" ODC pattern revealed by CO differs noticeably from the "anatomic" ODC pattern revealed by [^{3}H]proline; rows of thin-dark and wide-pale CO-staining were evident (three representative rows of darker ODC staining are marked by the arrows).[12,24] By overlapping CO-stained section with [^{3}H]proline-labeled section, using blood vessels as land-

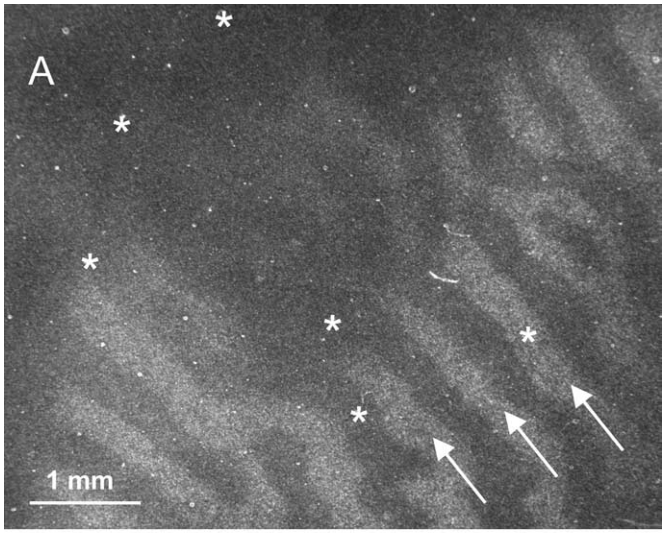

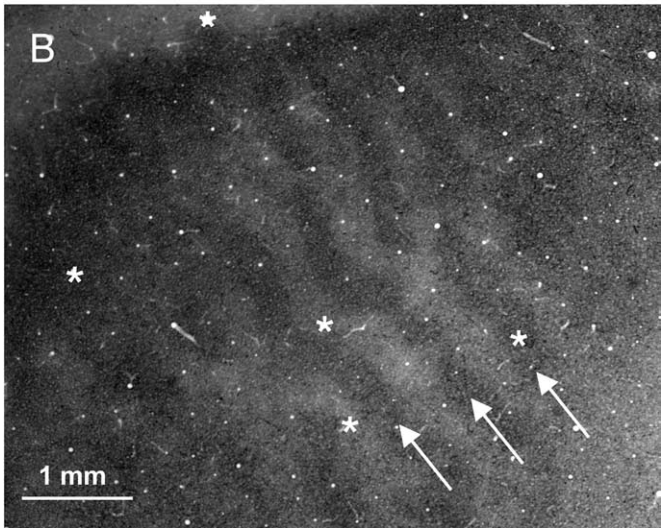

FIG 5. (A) Tangential sections through layer 4C of opercular V1 in naturally exotropic monkey PY who had strabismic amblyopia of the left eye. Top panel: section labeled with [^{3}H]proline. The ODCs of the proline injected right eye appear as pale stripes (white arrows). (B) Adjacent section stained with CO. Rows of thin dark and wide pale CO-staining are evident. Three representative rows of darker staining ODCs are marked by arrows. The CO-dark ODCs align with the proline-pale ODCs, corresponding to the preferred right eye. Radial blood vessels used for aligning the sections are indicated by asterisks.

marks (asterisks), we could determine that the CO-dark ODCs corresponded to [^{3}H]proline-pale ODCs and thus belonged to the preferred right eye. Inspection of sections through the opercular and calcarine cortex disclosed that both the central and the peripheral retinotopic regions of V1 exhibited the ODC inequality seen in Figure 5. Thin-dark CO stripes corresponded to the centers of the preferred eye ODCs, but wide-pale CO stripes corresponded to the entire width of the amblyopic eye ODCs *plus* the border strips of the preferred eye ODC.[24]

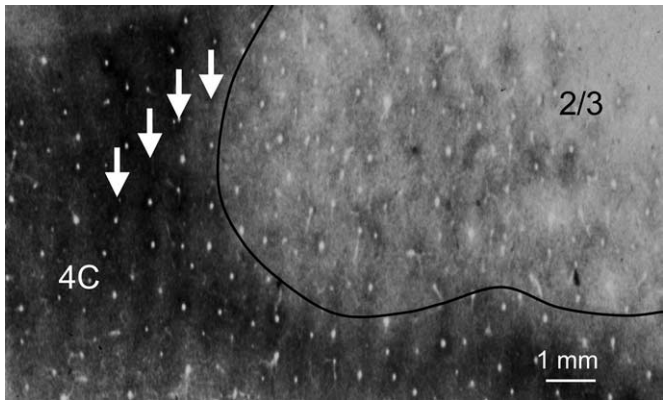

FIG 6. Tangential section through opercular V1 of ao-ET monkey RD who alternated fixation and had no amblyopia. The left and lower regions of this section traverse layer 4C, and the right upper regions layers 4B, 2, and 3. Alternate rows of darker (arrows) and lighter staining ODCs are visible in layer 4C. As in strabismic monkey JE, the darker staining ODCs in monkey RD belonged to the contralateral eye (ie, were driven by inputs from the nasal hemiretina). From the same region of cortex reported previously in Tychsen and Burkhalter, 1997, Figure 7B.

V1 Metabolic Labeling in Alternating Strabismus without Amblyopia

The thin-dark, wide-pale pattern of CO staining was also observed in sections through V1 of the two monkeys who had alternating esotropia without amblyopia. The suppression in these nonamblyopic animals conformed to a nasal-versus-temporal, rather than preferred-versus-amblyopic-eye rule in each hemisphere.[9] Figure 6 is a CO-stained section through opercular V1 in ao-ET monkey RD, cut parallel (flat or tangential) to the pial surface. The left lower regions of this section traverse layer 4C, and the right upper regions traverse layers 4B, 2, and 3. Alternate rows of thin-dark (arrows) and wide-pale ODCs were visible in layer 4C. The CO-staining characteristics of the optic disk representations and monocular crescents indicated that the darker staining stripes in each hemisphere corresponded to ODCs driven by the nasal hemiretinae. A similar, nasal-darker, temporal-paler CO pattern was observed in the right and left hemispheres of nat-ET monkey JE (not shown), who also had anterograde labeling of ODCs by injection of WGA-HRP into one eye. The CO stripe pattern in these animals was most conspicuous in the opercular cortex.

The bar graph of Figure 7 quantifies the difference in density of CO staining for ODCs in strabismic monkeys RD and JE. The normal monkey's ODCs revealed no interocular difference, whereas the two strabismic monkeys showed substantial differences in density of CO staining ($P < 0.01$) between alternating rows of ODCs. The difference between dark and light ODCs was comparable in the two strabismic animals, and in opercular and calcarine regions of V1.

Journal of AAPOS
Volume 9 Number 1 February 2005

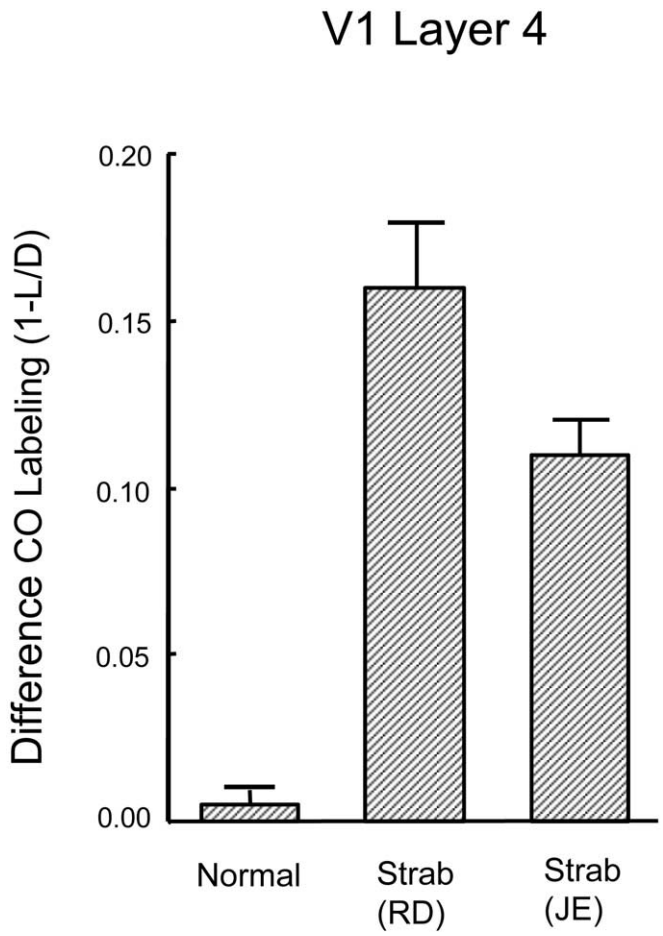

FIG 7. Metabolic suppression quantified as difference in density of CO staining for ODCs in strabismic monkeys RD and JE, compared with normal monkeys from our laboratory. The two strabismic monkeys, when compared with control monkeys, showed substantial differences in density of CO staining ($P < 0.01$) between ODCs of opposite ocularity. Modified from Tychsen and Burkhalter, 1997.

DISCUSSION

The main finding of the present study is that unrepaired strabismus in primates is associated with altered metabolic activity in the visual neurons at the input layer of V1, layer 4C. Our study revealed more pronounced metabolic suppression of ODCs when strabismus is combined with amblyopia. The abnormality in monkey cortex correlates with clinical observations in strabismic humans. Binocularity is impaired to a greater degree, and suppression tends to be more pronounced, in patients who have combined strabismus and amblyopia, as compared with strabismus alone (that is, alternating fixation). The metabolic abnormalities were found throughout V1, which is composed predominantly of neurons with binocular interactions. The suppression was not evident in the LGN, which is composed of neurons driven monocularly from each eye without binocular interaction. Our findings support the notion that abnormal binocular interaction in V1 leads to heightened competition between ODCs of opposite ocularity, with suppression of metabolic activity in opposite-eye ODCs. The results contribute to a growing body of knowledge on brain development and the devastating effects of unrepaired strabismus. The effects include an ~50% reduction in long-range, excitatory binocular horizontal connections joining ODCs of opposite ocularity.[3,4] Our results imply that in the presence of strabismus the remaining 50% of binocular connections (long-range, short-range, or a combination) mediate mainly inhibition.

Suppression of Monocular versus Binocular Zones within ODCs

Inequalities in CO staining of ODCs do not occur in normal primates unless one eye is deafferented for an extended period before death, by enucleation, lid suturing, or laser ablation of the optic nerve.[24,40] The abnormality of CO staining observed in the ODCs of the strabismic animals occurred spontaneously, ie, without any experimental, monocular deafferentation. The abnormality was characterized by thin dark stripes of intense staining alternating with wider pale stripes of weak staining. The abnormality represents zones of heightened versus reduced enzymatic neuronal activity, respectively.

Tychsen and Burkhalter reported metabolic suppression of V1 ODCs, evident as light and dark CO-stained stripes, in nonamblyopic monkeys with natural, infantile-onset esotropia.[3,9] They did not comment on center versus border zones of these "spontaneous stripes," noting only that they had "the exact periodicity of alternating rows of ODCs."[9] Fenstemaker et al also noted light and dark CO-stripes ("of approximately equal width") in V1 of two monkeys with alternating esotropia, produced by surgical manipulation of the extraocular muscles at age 9 days.[10] Horton and coworkers showed that the alterations of ODC CO-activity could be produced in monkeys at adult age if a fixation preference for one eye occurred as a result of artificial exotropia.[12] The Horton et al study also made novel and important discoveries about the CO-pattern in strabismic V1: the dark stripes of intense CO staining were always thinner than the anatomic width of ODCs and corresponded to the center zone of the preferred-eye columns, whereas the pale stripes of weak staining were always wide, corresponding to the entire width of the suppressed-eye column *plus* the binocular border zones of the neighboring, preferred-eye columns.[12,24] Thus, uncorrelated binocular activity in V1 leads to suppression, not only of columns belonging to the nonpreferred eye, but extends to include suppression of binocular border zone neurons within the columns of the preferred eye (Figure 8).

Suppression in Strabismus versus Strabismic Amblyopia

The thin-dark, wide-pale pattern observed in the four strabismic monkeys of the current report suggests a hierarchy of graded effect. The pattern was most striking in the monkeys with the largest-angle, unilateral strabismus

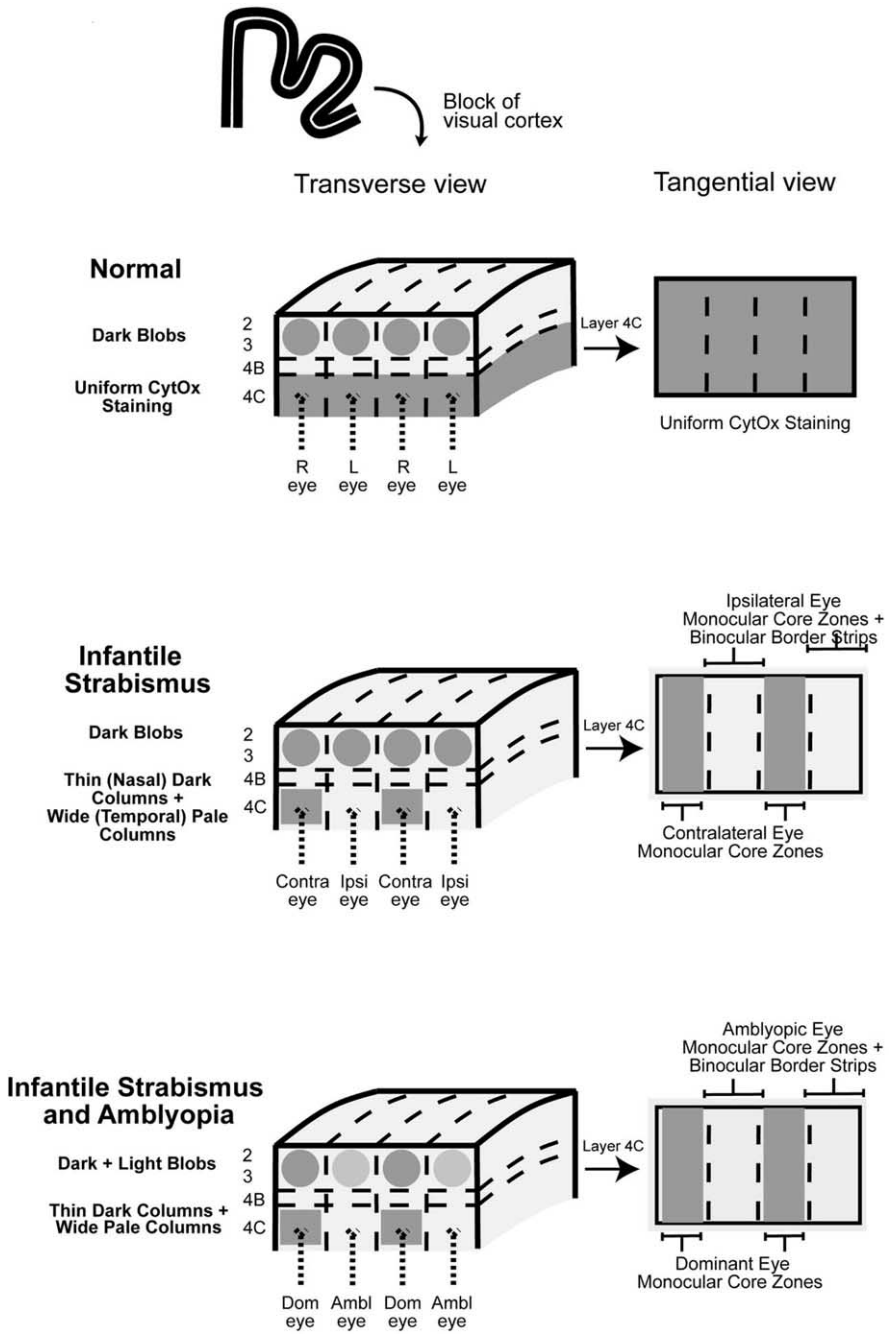

FIG 8. Summary of CO-staining patterns, indicative of metabolic suppression, in areas V1 of strabismic versus normal macaque monkeys. Normal: No metabolic suppression. Layer 4C stains uniformly for CO, and ODCs of each eye contain CO blobs or patches within layers 2/3, which also stain equally and are aligned with the center of the ODC. The tangential (flattened) sections through V1 layer 4C show no ODC stripes. Infantile Strabismus: Interocular suppression of ODCs driven by the ipsilateral eye in each V1. ODCs driven by the contralateral eye have higher metabolic activity, a narrow, darkly staining monocular core zone. The dark stripes alternate with wider pale stripes composed of the ipsilateral eye monocular core zone plus binocular border stripes. CO-blobs in layers 2/3 tend to stain uniformly. Infantile Strabismus and Amblyopia: Interocular suppression of ODCs driven by the amblyopic eye in each V1. ODCs driven by the dominant eye have higher metabolic activity, evident as a narrow, darkly staining monocular core zone. The dark stripes alternate with wider pale stripes composed of the amblyopic eye monocular core zone plus binocular border strips. CO-blobs in layer 2/3, driven by the amblyopic eye, stain less intensely.

combined with amblyopia (monkeys ZY and PY), and less pronounced in the monkeys with alternating, moderate, or small-angle strabismus and no amblyopia (monkeys JE and RD). Horton et al also noted more extensive CO-staining differences in strabismic monkeys with stronger unilateral fixation preferences.[12] The gradation in our animals corresponds to clinical observations in humans that sensorial suppression tends to be severe in the presence of early

onset, large-angle strabismus with dense amblyopia, and milder in microstrabismus without amblyopia.[41-43]

Nasotemporal Bias of Suppression

Psychophysical studies of the development of the hemifields in normal human infants indicate that temporal retina sensitivity matures slower than nasal retina sensitivity.[44,45] The nasotemporal asymmetry in sensitivity diminishes if the infant develops normal vision, but lower temporal sensitivity remains permanently if early binocular development is disrupted by strabismus or amblyopia[42,46,47] (for review, see ref. 9).

In the two strabismic animals (JE and RD) who alternated fixation, lower CO activity was apparent in ODCs driven by the ipsilateral eye in V1 of both the right and the left hemispheres (Figure 8). Ipsilateral inputs originate from the temporal hemiretinae of each eye, implying that inputs to V1 from the temporal hemiretinae are at a developmental disadvantage. Horton et al[12] observed a similar nasotemporal inequality of CO activity in four of five monkeys made exotropic at adult age. In Horton et al's study,[12] the suppression of temporal-retina-driven ODCs was limited to the calcarine cortex (peripheral visual field), but in monkeys JE and RD of the current study, the bias was evident within opercular (foveal) cortex. The human psychophysical findings, together with the monkey anatomic findings, reinforce the conclusion that abnormal binocular experience in early infancy unfairly punishes visual neurons that are slow to develop and fewer in number, that is, those driven by the temporal hemiretina.[9] The nasotemporal bias is inapparent in the presence of normal binocular vision, but persists and may be unmasked in adulthood if binocularity is disrupted by constant strabismus.

References

1. Hubel DH, Wiesel TN. Receptive fields and functional architecture of monkey striate cortex. J Physiol 1968;195:215-43.
2. Hubel DH, Wiesel TN. Anatomical demonstration of columns in the monkey striate cortex. Nature 1969;221:747-50.
3. Tychsen L, Burkhalter A. Neuroanatomic abnormalities of primary visual cortex in macaque monkeys with infantile esotropia: preliminary results. J Pediatr Ophthalmol Strabismus 1995;32:323-8.
4. Tychsen L, Wong AMF, Burkhalter A. Paucity of horizontal connections for binocular vision in V1 of naturally-strabismic macaques: cytochrome-oxidase compartment specificity. J Comp Neurol 2004; 474:261-75.
5. Jampolsky A. Characteristics of suppression in strabismus. Arch Ophthalmol 1955;54:683.
6. Pratt-Johnson JA, Tillson G. Suppression in strabismus—an update. Br J Ophthalmol 1984;68:174-8.
7. Hirsch JA, Gilbert CD. Synaptic physiology of horizontal connections in primary visual cortex. J Neurosci 1991;11:1800-9.
8. Weliky M, Kandler K, Fitzpatrick D, Katz LC. Patterns of excitation and inhibition evoked by horizontal connections in visual cortex share a common relationship to orientation columns. Neuron 1995; 15:541-52.
9. Tychsen L, Burkhalter A. Nasotemporal asymmetries in V1: ocular dominance columns of infant, adult, and strabismic macaque monkeys. J Comp Neurol 1997;388:32-46.
10. Fenstemaker SB, Kiorpes L, Movshon JA. Effects of experimental strabismus on the architecture of macaque monkey striate cortex. J Comp Neurol 2001;438:300-17.
11. Horton JC, Hocking DR, Kiorpes L. Pattern of ocular dominance columns and cytochrome oxidase activity in a macaque monkey with naturally occurring anisometropic amblyopia. Vis Neurosci 1997;14: 681-9.
12. Horton JC, Hocking DR, Adams DL. Metabolic mapping of suppression scotomas in striate cortex of macaques with experimental strabismus. J Neurosci 1999;19:7111-29.
13. Tychsen L, Scott C. Maldevelopment of convergence eye movements in macaque monkeys with small and large-angle infantile esotropia. Invest Ophthalmol Vis Sci 2003;44:3358-68.
14. Zipf RF. Binocular fixation pattern. Arch Ophthalmol 1976; 94:401-5.
15. Teller DY, Regal DM, Videen TO, Pulos E. Development of visual acuity in infant monkey (*Macaca nemestrina*) during early postnatal weeks. Vision Res 1978;18:561-6.
16. Finney DJ. Probit Analysis. Cambridge, UK: Cambridge Univ. Press; 1971.
17. Norcia AM, Tyler CW. Spatial frequency sweep VEP: visual acuity during the first year of life. Vision Res 1985;25:1399-1408.
18. O'Dell C, Boothe RG. The development of stereoacuity in infant rhesus monkeys. Vision Res 1997;37:2675-84.
19. Foeller P, Tychsen L. Eye movement training and recording in alert macaque monkeys: 1. Operant visual conditioning. 2. Magnetic search coil and head restraint surgical implantation. 3. Calibration and recording. Strabismus 2002;10:5-22.
20. Robinson DA. A method of measuring eye movement using a scleral search coil in a magnetic field. IEEE Trans Biomed Electron 1963; 10:137-45.
21. Fuchs AF. Saccadic and smooth pursuit eye movements in the monkey. J Physiol 1967;191:609-31.
22. Wiesel TN, Hubel DH. Ordered arrangement of orientation columns in monkeys lacking visual experience. J Comp Neurol 1974; 158:307-18.
23. Hoyt WF, Luis O. Visual fiber anatomy in the infrageniculate pathway of the primate. Arch Ophthalmol 1962;68:124-36.
24. Horton JC, Hocking DR. Monocular core zones and binocular border strips in primate striate cortex revealed by the contrasting effects of enucleation, eyelid suture, and retinal laser lesions on cytochrome oxidase activity. J Neurosci 1998;18:5433-55.
25. Olavarria J, Van Sluyters RC. Unfolding and flattening the cortex of gyrencephalic brains. J Neurosci Methods 1985;15:191-202.
26. Sincich LC, Adams DL, Horton JC. Complete flatmounting of the macaque cerebral cortex. Vis Neurosci 2003;20:663-86.
27. Gibson AR, Hansma DI, Houk JC, Robinson FR. A sensitive low artifact TMB procedure for the demonstration of WGA-HRP in the CNS. Brain Res 1984;298:235-41.
28. Mesulam MM. Tetramethyl benzidine for horseradish peroxidase neurohistochemistry: a non-carcinogenic blue reaction product with superior sensitivity for visualizing neural afferents and efferents. J Histochem Cytochem 1978;26:106.
29. Tootell RBH, Hamilton SL, Silverman MS, Switkes E. Functional anatomy of macaque striate cortex. I. Ocular dominance, binocular interactions, and baseline conditions. J Neurosci 1988;8:1500-30.
30. Hevner RF, Wong-Riley MTT. Mitochondrial and nuclear gene expression for cytochrome oxidase subunits are disproportionately regulated by functional activity in neurons. J Neurosci 1993;13:1805-19.
31. Busettini C, Miles FA, Krauzlis RJ. Short-latency disparity vergence responses and their dependence on a prior saccadic eye movement. J Neurophysiol 1996;75:1392-1410.
32. Tychsen L. Infantile esotropia: current neurophysiologic concepts. In: Rosenbaum AL, Santiago AP, editors. Clinical Strabismus Management. Philadelphia (PA): Saunders, 1999. p. 117-38.

33. Horton JC, Hubel DH. Regular patchy distribution of cytochrome oxidase staining in primary visual cortex of macaque monkey. Nature 1981;292:762-4.
34. Horton JC. Cytochrome oxidase patches: a new cytoarchitectonic feature of monkey visual cortex. Phil Trans R Soc Lond 1984;304: 199-253.
35. Van Essen DC, Newsome WT, Maunsell JHR. The visual field representation in striate cortex of the macaque monkey: asymmetries, anisotropies, and individual variability. Vision Res 1984;24: 429-48.
36. LeVay S, Connolly M, Houde J, Van Essen DC. The complete pattern of ocular dominance stripes in the striate cortex and visual field of the macaque monkey. J Neurosci 1985;5:486-501.
37. Tootell RBH, Switkes E, Silverman MS, Hamilton SL. Functional anatomy of macaque striate cortex. II. retinotopic organization. J Neurosci 1988;8:1531-68.
38. Le Gros Clark WE. The laminar organization and cell content of the lateral geniculate body in the monkey. J Anat 1941;75:419-33.
39. Connolly M, Van Essen DC. The representation of the visual field in parvicellular and magnocellular layers of the lateral geniculate nucleus in the macaque monkey. J Comp Neurol 1984;226:544-64.
40. Horton JC, Hocking DR. Effect of early monocular enucleation upon ocular dominance columns and cytochrome oxidase activity in monkey and human visual cortex. Vis Neurosci 1998;15:289-303.
41. Sireteanu R. Binocular vision in strabismic humans with alternating fixation. Vision Res 1982;22:889-96.
42. Sireteanu R, Fronius M. Naso-temporal asymmetries in human amblyopia: consequence of long-term interocular suppression. Vision Res 1982;21:1055-63.
43. Birch EE, Stager DR, Berry P, Everett ME. Prospective assessment of acuity and stereopsis in amblyopic infantile esotropes following early surgery. Invest Ophthalmol Vis Sci 1990;31:758-65.
44. Lewis TL, Maurer D, Blackburn K. The development of young infants' ability to detect stimuli in the nasal visual field. Vision Res 1985;25:943-50.
45. Lewis TL, Maurer D. The development of the temporal and nasal visual fields during infancy. Vision Res 1992;32:903-11.
46. Sireteanu R, Fronius M. Visual field losses in strabismic amblyopes. Klin Monatsbl Augenheilkd 1989;194:261-9.
47. Bowering ER, Maurer D, Lewis TL, Brent HP. Sensitivity in the nasal and temporal hemifields in children treated for cataract. Invest Ophthalmol Vis Sci 1993;34:3501-9.

An Eye on the Arts – The Arts on the Eye

As I grow older I become less interested in travel to other parts of the world. There is so much absolute beauty along the California coast that I could work for a century, exploring with eye and lens. Photographers who frequently travel photograph with less than full knowledge of their subjects. I believe one must live in a region for a considerable time and absorb its character and spirit before the work can truly reflect the experience of the place. In my own case, hasty visits have usually resulted in inconsequential images; perhaps an occasional flash of insight, or a remembrance of an earlier place or time helped in visualizing a photograph. But most often I have grasped for some evanescent image only to find it a hollow recording of the subject because I really did not see or understand what was before me.

—Ansel Adams (from *Ansel Adams: An Autobiography*)